

LIFETIME MEASUREMENTS OF EXCITED STATES IN EXOTIC NUCLEI PRODUCED IN REACTIONS AT INTERMEDIATE ENERGIES*

K. STAROSTA^{a,b}, P. ADRICH^a, A. DEWALD^c, D. MILLER^{a,b}
V. MOELLER^{b,d}, C. VAMAN^b, P. VOSS^{a,b}

^aNational Superconducting Cyclotron Laboratory, East Lansing, MI 48824, USA

^bDepartment of Physics, Michigan State University, East Lansing, MI 48824, USA

^cInstitute for Nuclear Physics, Universität zu Köln, Köln, 50937 Germany

^dCavendish Laboratory, Cambridge University, Cambridge, CB3 0HE, UK

(Received November 13, 2008)

The current status and outlook for the Doppler-effect based lifetime measurements program at the National Superconducting Cyclotron Laboratory is presented, including the impact of the Digital Data Acquisition System which provides gamma-ray tracking capabilities for the Segmented Germanium Array.

PACS numbers: 21.10Tg, 23.20–g, 25.60.–t, 29.38Db

1. Introduction

The Recoil Distance Method (RDM) and related Doppler Shift Attenuation Method (DSAM) following Coulomb excitations, knock-out, and fragmentation at intermediate energies of ~ 100 MeV/ u hold the promise of providing lifetime information for excited states in a wide range of unstable nuclei. Recently, the RDM was implemented at the National Superconducting Cyclotron Laboratory (NSCL) at Michigan State University [1] using the customized Köln plunger device [2] and a unique combination of state-of-the-art instruments available there. The results for two RDM experimental schemes with fast beams are presented. Absolute transition rates of the first 2^+ state in ^{110}Pd and ^{114}Pd were measured using RDM following projectile Coulomb excitations [3]. The ^{110}Pd experiment served to check the novel experimental technique as well as the method used for data analysis, which is based on the examination of gamma-ray line shapes. Whereas the measured

* Presented at the Zakopane Conference on Nuclear Physics, September 1–7, 2008, Zakopane, Poland.

$B(E2)$ for ^{110}Pd agrees very well with the literature value, the $B(E2)$ for ^{114}Pd differs considerably from the evaluated value. The new experimental data on neutron-rich Pd isotopes validate a novel concept, called valence proton symmetry, which allows for the extrapolation of the transition rates to very neutron rich nuclei.

In a separate experiment, absolute transition rates were measured for the first and second 2^+ states in $N = Z$ ^{64}Ge , far from the line of nuclear stability [4]. Levels of interest were populated via an intermediate energy single-neutron knock-out reaction. The experimental results were found to be in excellent agreement with large-scale Shell Model calculations applying the recently developed GXPf1A interactions. The future application of the Doppler-shift methods at the NSCL will benefit significantly from the implementation of the Digital Data Acquisition System (DDAS) [5] which provides gamma-ray tracking capabilities for the Segmented Germanium Array (SeGA) [6].

2. Experimental method

In a typical plunger experiment at the NSCL, the rare isotopes of interest (produced in a fragmentation reaction) impinge with a velocity $v/c \approx 0.3$ on a secondary plunger target as shown in Fig. 1. The excited projectile-like reaction residue emerges from the target and decays in flight by γ -ray emission after traversing a distance that depends on both the velocity of the residue and the lifetime of the excited state. A degrader is positioned downstream from the plunger target to reduce the velocity of the residue to $v/c \approx 0.2$. Depending on whether the in-flight γ -decay occurred before or after the degrader, the γ -rays exhibit different Doppler shifts. Consequently, the measured γ -ray spectrum contains two peaks for each transition, as shown in the right side of Fig. 1. The lifetime of the state can be inferred from the relative intensities of the peaks as a function of the target-degrader distance if the velocity of the residue is known. The excited states of interest can be populated using different reaction mechanisms *e.g.* electromagnetic excitation, fragmentation, or nucleon knockout.

In experiments with secondary beams of rare isotopes at the NSCL the plunger device is located at the target position of the S800 spectrograph [7] and is surrounded by 15 detectors of SeGA, an array of high-purity germanium 32-fold segmented detectors [6]. The SeGA configuration for Doppler-shift experiments consist of two rings of 7 and 8 detectors placed at 30° and 140° with respect to the beam axis, respectively. Both the incoming projectile (usually delivered as a cocktail beam composed of several isotopes of similar mass to charge ratio) and the outgoing projectile-like reaction residue are identified event by event and the γ -rays are measured in coincidence with

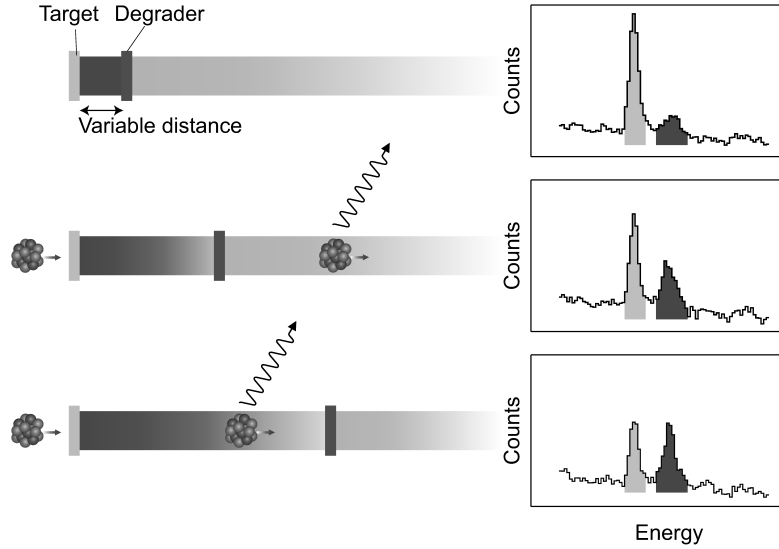


Fig. 1. Left: Schematic arrangement of the excitation target (light gray) and the degrader (dark gray) in a plunger lifetime measurement with a short (top), intermediate (middle), and a long (bottom) flight path. The regions for decay upstream and downstream from the degrader are marked in dark and light gray and correspond to ion velocities of $v/c \approx 0.3$ and $v/c \approx 0.2$, respectively. Right: Experimental spectra obtained using the test setup at NSCL [1]; peaks marked with dark and light gray correspond to the reaction products decaying upstream and downstream of the degrader, respectively.

the heavy ions. This results in significant reduction of the background in the γ -ray spectra and furthermore allows simultaneous measurements of transition lifetimes in many nuclei produced in different reaction channels. The constituents of the secondary cocktail beam are identified by their time of flight measured over a long distance while the secondary reaction residues are transported to the focal plane of the S800 spectrograph and are identified by means of time of flight and energy loss measurements.

In an experiment with low-intensity exotic beams, experimental conditions have to be balanced such that the reaction rate in the target is maximized while the peaks in the γ -ray energy spectrum corresponding to decays before and after the degrader are well separated in energy. This is a complex optimization task which requires input of reaction cross sections, beam intensity and momentum dispersion, stopping powers of materials considered for the target and degrader, geometry and response of the γ -ray detector, and an estimate of the expected range for the lifetime of the state of interest. A Geant4-based [8] simulation program [9] was developed to facilitate this optimization process.

To analyze the data, the procedure was developed [3, 4] taking into account peak shape as well as intensity ratios measured at each target-degrader separation. The calculations treat the process of γ -radiation from excited nuclei relativistically. The change of the detection angle with respect to the velocity of the nucleus and the locus of the γ -ray emission are taken into account. Attention was also paid to the decays occurring behind the degrader for relatively long lifetimes. In this way, the total line-shape, consisting of the peaks generated by emissions in flight (fully-shifted and degraded) and of the contributions from emissions while slowing down in the target or degrader, can be calculated as a function of the lifetime τ and a factor that normalizes the simulation to the data. A fitting procedure leads to the determination of these quantities for each separation distance. The test case of ^{62}Zn from experiment [4] is shown in Fig. 2. An excellent agreement between the measured lifetime of the $2_1^+ \rightarrow 0_1^+$ transition of $\tau = 4.2(7)$ ps and the literature value of $4.2(3)$ [10] resulted from these fits. The corresponding fitting and analysis procedures are implemented in the simulation code described in [9].

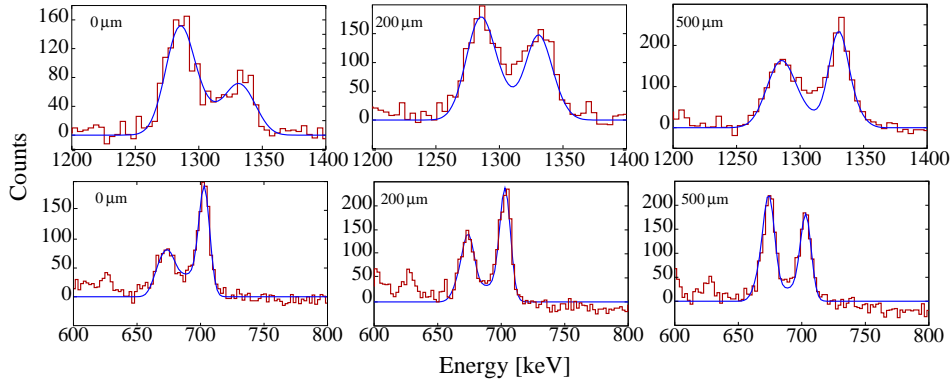


Fig. 2. Simultaneous fit of spectra for ^{62}Zn at 30° (top) and 140° (bottom) rings of SeGA from the experiment [4]. The corresponding target-degrader separations are indicated. The Doppler corrections account for the detector segmentation but not for the angular position of the detector in the array.

3. Collectivity of neutron-rich Pd nuclei from Coulex RDM

A transition from almost spherical Sn towards vibrational Cd and moderately deformed Pd and Ru nuclei is observed for neutron-rich nuclei below $Z = 50$. In this region, triaxiality and gamma-softness are predicted to play an important role in shape evolution [11]. The neutron-rich Pd nuclei are of special interest because a prolate-to-oblate shape transition is expected from

mean field calculations [12]. Whereas the energy spectra of the neutron-rich palladium isotopes develop smoothly with neutron number N , the measured $B(E2; 2_1^+ \rightarrow 0_1^+)$ values for $^{112,114}\text{Pd}$ [13] deviate from the prediction made by Kim *et al.* [14] and the Grodzins relation [15] (see Fig. 1 of Ref. [3]).

In experiment reported in [3] addressing this discrepancy, a 120 MeV/ u primary beam of ^{124}Sn was delivered from the K500/K1200 coupled cyclotrons and directed on a ^9Be production target positioned at the object point of the A1900 fragment separator [16]. The secondary beams were produced using in-flight fragmentation and purified in the A1900 via energy loss separation in an Al wedge. Two cocktails consisting of ^{108}Rh , ^{110}Pd , and ^{112}Ag isotopes for the ^{110}Pd settings and of ^{112}Rh , ^{114}Pd , and ^{116}Ag isotopes for the ^{114}Pd settings were delivered to the S800 spectrograph. Particle identification after the plunger's target and the degrader foils was made on an event by event basis using the time of flight measured via a diamond detector [17] positioned in the object location of the S800 and by a plastic scintillator in the focal plane of the S800. Energy loss signals of reacted Pd projectiles were measured with the ionization chamber of the S800 focal plane while scattering angle information was provided by two CRDC detectors [18]. Particle identification in the Coulex experiment is facilitated by the fact that the beam incoming to and outgoing from the plunger target is the same. The intensity of the ^{110}Pd and ^{114}Pd beams was 11000 pps/ pnA and 1500 pps/ pnA , respectively; for ^{124}Sn , 1.5 pnA of primary beam is typically achieved at the NSCL.

Fig. 2 of Ref. [3] shows an excellent agreement between the data for the first excited 2^+ state in ^{114}Pd and the results of the simultaneous fit of the lineshapes at forward and backward angles. The lifetimes of the first 2^+ states in ^{110}Pd and ^{114}Pd have been determined from the fitting procedure. For the 2_1^+ lifetime in ^{110}Pd , which is quite well known, a value of $\tau = 67(8)$ ps was obtained which coincides with the average value from the literature. In contrast, the lifetime of the 2_1^+ level in ^{114}Pd , determined to be $\tau = 118(20)$ ps, is more than two times smaller than the previous result [13, 19]. This is further supported by a measurement performed for ^{112}Pd and ^{114}Pd by Mach *et al.* at JYFL, Jyväskylä using fast timing technique as outlined in the 2003 JYFL Annual Laboratory Report [20]. The 2_1^+ lifetime in ^{114}Pd from Ref. [20] perfectly agrees with our result, while the corresponding value for ^{112}Pd is in conflict with the one given in Ref. [13].

Since the actual interest in nuclear structure concentrates on very neutron-rich nuclei, it is appropriate to develop methods for extrapolating nuclear observables like the energy spectrum and absolute transition rates towards the neutron dripline. The predictions of 2^+ lifetimes in Pd isotopes at large isospin values can be made based on a concept called valence proton symmetry (VPS), which is a special case of the valence correlation

scheme (VCS) introduced in [21]. Nuclei $({}_{Z_x}^{A_x}X_{N_x})$ and $({}_{Z_y}^{A_y}Y_{N_y})$ can be considered as valence-proton symmetric if $N_x = N_y$, $Z_x < Z_m < Z_y$ and $|Z_m - Z_x| = |Z_m - Z_y| = N_\pi$ where Z_m is the magic proton number closest to Z_x and Z_y and N_π is the valence proton number. Nuclei with valence proton symmetry form pairs (called later VPS-pairs) where each partner is supposed to have the same nuclear structure, exhibited, in an ideal case, by identical excitation spectra and transition probabilities. In real nuclei this symmetry is broken to some extent, but the gross features of the nuclear structure should be preserved.

Pd and Xe nuclei with identical neutron numbers N form VPS-pairs and thus the same deformation or collectivity is expected for these nuclei, exhibited by similar energies of the low-lying excited states and similar B(E2) transition strengths. The similarity of the experimental data for the Xe and Pd isotopes with identical neutron numbers reveals the equivalence of the valence space in these nuclei. Some differences remain, mainly due to the mass and charge differences which break the VPS to some extent. For the B(E2) values the effect of symmetry breaking can be compensated by applying the scaling factors $S(N, 50) = (Z_{\text{Pd}}/Z_{\text{Xe}})^2 * (A_{\text{Pd}}/A_{\text{Xe}}) = (46/54)^2 * (46 + N)/(54 + N)$ where N is the neutron number. Using these scaling factors for the B(E2)'s in the Xe isotopes the agreement of the experimental values of the two isotopic chains Pd and Xe becomes evident, as shown in Fig. 3. In this figure the scaled B(E2) values of Xe isotopes are compared with B(E2) values of Pd isotopes. For the VPS-pairs (${}^{114}\text{Xe}/{}^{106}\text{Pd}$), (${}^{116}\text{Xe}/{}^{108}\text{Pd}$), (${}^{118}\text{Xe}/{}^{110}\text{Pd}$), and (${}^{122}\text{Xe}/{}^{114}\text{Pd}$), the experimental values

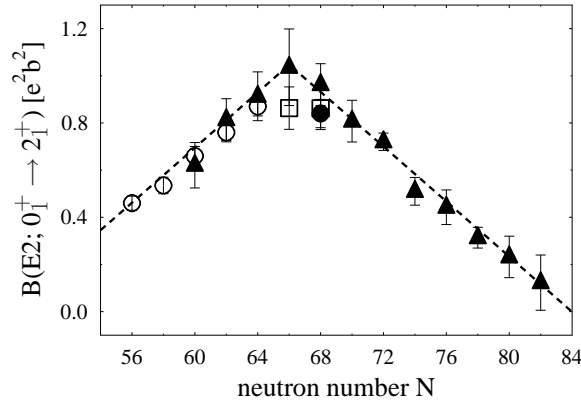


Fig. 3. $B(\text{E}2; 0_1^+ \rightarrow 2_1^+)$ values of Pd isotopes (dots) compared with scaled values of the corresponding Xe VPS partners (triangles) using the scaling factor $S = (Z_{\text{Pd}}/Z_{\text{Xe}})^2 * (A_{\text{Pd}}/A_{\text{Xe}})$. Open boxes are for ${}^{112,114}\text{Pd}$ results from Ref. [20], a full dot is for the ${}^{114}\text{Pd}$ result presented here.

agree within the errors. Only for ($^{120}\text{Xe}/^{112}\text{Pd}$) do the values deviate a bit more, but are still very close. For the Xe nuclei with $62 < N < 90$, a lot of experimental data are available to determine the nuclear structure; thus these can be used to predict structure properties of the corresponding very neutron-rich Pd VPS-partners.

4. Structure of $N = Z$ ^{64}Ge from knock-out RDM

Experiments involving $N = Z$ nuclei play a vital role in the understanding of nuclear structure. Along the $N = Z$ line, protons and neutrons occupy the same shell-model orbitals. The resulting overlap of nucleon wave functions leads to an amplification of the residual proton-neutron interactions. In nuclei with $28 < N = Z < 50$, large shell gaps open simultaneously for prolate and oblate quadrupole deformations. This region is a subject of vigorous experimental studies due to a remarkable diversity of shapes. Variations in the excitation energy of low-lying states in this region are often used to analyze the evolution of structure away from the doubly-magic ^{56}Ni core. However, electromagnetic transition rates are recognized as providing a more sensitive probe of collectivity and deformation.

Successful application of the RDM opens up new possibilities for lifetime measurements of excited states in $N = Z$ nuclei at fragmentation facilities. In the experiment reported in [4], states of interest were populated via an intermediate-energy single neutron knock-out from beams of ^{65}Ge and ^{63}Zn . The transition rates in ^{62}Zn are known from measurements in stable beam facilities [10] and served as a consistency check for the method while transitions in $N = Z$ ^{64}Ge were measured for the first time. The beam impinging on the plunger target-degrader was delivered as a cocktail comprised of 5% ^{65}Ge , 35% ^{64}Ga , 52% ^{63}Zn and 8% ^{62}Cu and was produced via in-flight projectile fragmentation of ^{78}Kr at 150 MeV/ u . The constituents of the incoming beam were identified on an event by event basis from the time of flight between the K1200 cyclotron and a diamond timing detector [17] in the object of the S800 spectrograph. The use of the radiation-hard diamond for particle identification was crucial to handle the $\sim 10^6$ particle-per-second rate of the incoming beam. The quality of the identification was sufficient to completely separate incoming beam components. The mass and charge of the products from reactions on the plunger target and degrader were extracted on an event by event basis from the time of flight and energy loss information. The time of flight was measured between the diamond detector in the object of the S800 and the E1 plastic scintillator in the S800 focal plane. The energy loss measurement was performed in the ionization chamber at the S800 focal plane [18]. In the off-line analysis the outgoing reaction products were identified separately for each component of the incoming cocktail beam.

From the measured lifetimes and data in Refs. [10] and [22] experimental observables were extracted and compared to the Shell Model GXFP1A calculations as summarized in Table I. The canonical effective charges of $e_p = 1.5 e$ and $e_n = 0.5 e$ were used for the B(E2) calculations. It should be stressed that the agreement between calculated and observed excitation energies for $N = Z$ ^{64}Ge is better than 50 keV, while the transition rates are reproduced within the experimental errors, except for the weak $2_2^+ \rightarrow 0_1^+$ transition. A similar level of agreement is reached for ^{62}Zn . In both cases, the theory predicts a negative and positive quadrupole moment for the 2_1^+ and the 2_2^+ state, respectively. Further theoretical analysis presented in [4] suggests that ^{64}Ge is a collective γ -soft anharmonic vibrator.

TABLE I

Comparison between the experimental data and the GXFP1A Shell Model calculations for ^{64}Ge and ^{62}Zn .

Nucl.	Observable	Exp.	Th.	Nucl.	Exp.	Th.	Unit
^{64}Ge	$E(2_1^+)$	0.902	0.938	^{62}Zn	0.954	1.012	MeV
^{64}Ge	$E(0_2^+)$		1.353				MeV
^{64}Ge	$E(2_2^+)$	1.579	1.559	^{62}Zn	1.805	1.908	MeV
^{64}Ge	$E(4_1^+)$	2.053	1.995				MeV
^{64}Ge	$B(E2, 2_1^+ \rightarrow 0_1^+)$	410(60)	406	^{62}Zn	250(18)	295	$e^2\text{fm}^4$
^{64}Ge	$B(E2, 2_2^+ \rightarrow 2_1^+)$	620(210)	610	^{62}Zn	290(50)	231	$e^2\text{fm}^4$
^{64}Ge	$B(E2, 2_2^+ \rightarrow 0_1^+)$	1.5(5)	14	^{62}Zn	4.5(7)	11	$e^2\text{fm}^4$
^{64}Ge	$B(E2, 0_2^+ \rightarrow 2_1^+)$		483				$e^2\text{fm}^4$
^{64}Ge	$B(E2, 0_2^+ \rightarrow 2_2^+)$		12				$e^2\text{fm}^4$
^{64}Ge	$B(E2, 4_1^+ \rightarrow 2_1^+)$		674				$e^2\text{fm}^4$
^{64}Ge	$B(E2, 4_1^+ \rightarrow 2_2^+)$		9				$e^2\text{fm}^4$
^{64}Ge	$Q(2_1^+)$		-18.6	^{62}Zn		-22.3	efm^2
^{64}Ge	$Q(2_2^+)$		+18.5	^{62}Zn		+13.8	efm^2

5. Perspectives for DSAM experiments with fast beams

The peak-shape calculations used in the analysis of the plunger data prompted investigation of DSAM experiments with fast beams from fragmentation. DSAM can be applied to measure lifetimes of excited states which are comparable to the time required to traverse the excitation target used in the experiment. In particular, the data on ^{104}Cd and ^{112}Sn from experiment [23] have been analyzed with a specific application of the Geant4 simulation code described in [9]. In this experiment a $\sim 110\mu\text{m}$ thick ^{197}Au target was used for Coulomb excitation of the incoming cocktail beam; the corresponding crossing time was ~ 1 ps. A classic SeGA configuration with

7 and 10 detectors in the 37° and 90° rings in the laboratory reference frame, respectively, was used to detect γ -rays emitted in the de-excitation process. Reaction residues were identified using the methods discussed above.

First, simulations were performed for ^{104}Cd which has a lifetime of the 2_1^+ state significantly longer than the 1 ps target crossing time. The measured and calculated spectra showed a very good agreement for the simultaneous fit of the γ -ray excitation peak observed at 37° and 90° rings of SeGA as well as for the particle energy and angle spectra measured by the S800. Next, a χ^2 minimization was performed for the corresponding spectra in ^{112}Sn as a function of the lifetime of the first excited state. From this analysis a minimum was found at a reasonable value of $\tau \sim 300$ fs, however, the shape of the χ^2 function indicated a strong correlation between the lifetime of interest and the velocity of the incoming beam. Indeed the velocity of the incoming beam defines the shape of a gamma-ray peak at the largest Doppler shift and has a direct impact on the lineshape. Uncertainty of the beam velocity in this experiment was 1%, which corresponds to 4 keV uncertainty in defining the high energy tail of the 1256 keV gamma-ray transition at 37° . The analysis indicates that while the DSAM experiments are feasible, special attention has to be paid to the beam properties as well as the geometry of the setup for gamma-ray detection. In particular, for the application at the NSCL, the plunger SeGA configuration provides significantly higher sensitivity than that of classic SeGA, and a dedicated measurement of velocity profile for the incoming beam is needed to extract reliable and accurate DSAM lifetime information.

6. Expected impact of gamma-ray tracking

Current efforts of the authors are concentrated on the implementation of gamma-ray tracking in SeGA detectors enabled by the application of the digital signal processing from the DDAS [5]. Gamma-ray tracking combined with the tracking of heavy ions in the S800 offers an opportunity to significantly improve gamma-ray energy resolution in measurements at the NSCL through more accurate Doppler corrections. This will have a direct impact on the sensitivity of Doppler-shift based lifetime measurements. First, improved gamma-ray resolution allows for thinner degraders to be used in plunger measurements; as a result access to shorter lifetimes is possible. Moreover, measurements with multiple degraders can be envisioned, allowing for a lifetime to be extracted without a need to change the target-degrader distance. Also, better energy resolution opens an opportunity for efficient coincidence measurements which can eliminate feeding corrections present in RDM knock-out and fragmentation schemes. All of the above will play a significant role in pushing the precision lifetime measurements towards the neutron drip-line.

7. Summary and conclusions

The RDM and DSAM Doppler-shift techniques are largely model and reaction mechanism independent, and thus can be used as a precision tool to extract electromagnetic transition rates for nuclei of interest. Relative measurements of RDM and DSAM can provide a reliable probe of other methods which are based on absolute cross section measurements such as Coulomb excitations. Doppler-shift methods implemented at the NSCL for Coulex, knock-out, and fragmentation reaction products hold the promise of reaching far from stability and providing reliable lifetime information for intermediate-spin excited states in a wide range of nuclei.

REFERENCES

- [1] A. Chester *et al.*, *Nucl. Instrum. Methods* **A562**, 230 (2006).
- [2] A. Dewald *et al.*, GSI Scientific Report 2005, p. 38, (2006).
- [3] A. Dewald *et al.*, *Phys. Rev.* **C78**, 051302 (2008).
- [4] K. Starosta *et al.*, *Phys. Rev. Lett.* **99**, 042503 (2007).
- [5] W. Henning *et al.*, *Nucl. Instrum. Methods* **B261**, 1000 (2007).
- [6] W. Mueller *et al.*, *Nucl. Instrum. Methods* **A466**, 492 (2001).
- [7] D. Bazin *et al.*, *Nucl. Instrum. Methods* **B204**, 629 (2003).
- [8] S. Agostinelli *et al.*, *Nucl. Instrum. Methods* **A506**, 250 (2003).
- [9] P. Adrich *et al.*, *Nucl. Instrum. Methods* **A598**, 454 (2009).
- [10] H. Junde, B. Singh, *Nuclear Data Sheets* **91**, 317 (2000).
- [11] J. Skalski *et al.*, *Nucl. Phys.* **A617**, 282 (1997).
- [12] P. Möller *et al.*, *At. Data Nucl. Data Tables* **59**, 185 (1995).
- [13] G. Mamane *et al.*, *Nucl. Phys.* **A454**, 213 (1986).
- [14] K.-H. Kim *et al.*, *Nucl. Phys.* **A604**, 163 (1996).
- [15] L. Grodzins, *Phys. Lett.* **2**, 88 (1962).
- [16] D.J. Morrissey *et al.*, *Nucl. Instrum. Methods* **B204**, 90 (2003).
- [17] A. Stolz *et al.*, *Nucl. Instrum. Methods* **B241**, 858 (2005).
- [18] J. Yurkon *et al.*, *Nucl. Instrum. Methods* **A422**, 291 (1999).
- [19] J. Blachot, *Nuclear Data Sheets* **97**, 593 (2002).
- [20] H. Mach *et al.*, *JYFL Annual Report* (2003).
- [21] R.F. Casten, N.V. Zamfir, *Phys. Rev. Lett.* **70**, 402 (1993).
- [22] B. Singh, *Nuclear Data Sheets* **78**, 395 (1996).
- [23] C. Vaman *et al.*, *Phys. Rev. Lett.* **99**, 162501 (2007).